International Journal of Automotive Technology, Vol. 7, No. 6, pp. 749–756 (2006)

1229–9138/2006/030–14

COMPLEX STOCHASTIC WHEELBASE PREVIEW CONTROL AND SIMULATION OF A SEMI-ACTIVE MOTORCYCLE SUSPENSION BASED ON HIERARCHICAL MODELING METHOD

L. WU* and H.-L. CHEN

Institute of Sound and Vibration Control, Xi'an Jiaotong University, 28 Xianning Xilu Road, Xi'an 710049, Shannxi Province, China

(Received 3 November 2005; Revised 2 June 2006)

ABSTRACT–This paper presents a complex stochastic wheelbase preview control method of a motorcycle suspension based on hierarchical modeling method. As usual, a vehicle suspension system is controlled as a whole body. In this method, a motorcycle suspension with five Degrees of Freedom (DOF) is dealt with two local independent 2-DOF suspensions according to the hierarchical modeling method. The central dynamic equations that harmonize local relations are deduced. The vertical and pitch accelerations of the suspension center are treated as center control objects, and two local semi-active control forces can be obtained. In example, a real time Linear Quadratic Gaussian (LQG) algorithm is adopted for the front suspension and the combination of the wheelbase preview and LQG control method is designed for the rear suspension. The results of simulation show that the control strategy has less calculating time and is convenient to adopt different control strategies for front and rear suspensions. The method proposed in this paper provides a new way for the vibration control of multi-wheel vehicles.

KEY WORDS : Hierarchical modeling method, Motorcycle suspension, Semi-active control, Wheelbase preview

1. INTRODUCTION

A vehicle suspension system is an important part of a vehicle. It can be classified into passive systems, active systems and semi-active systems. In recent years, the semi-active suspension systems based on magneto-rheological fluid (MRF) dampers can generate desired damping force while they use lower voltage or current at the same time. Hence the semi-active suspension systems are getting more attention (Kok *et al.*, 1997; Ericksen and Gordaninejad, 2003).

In conventional design, a vehicle suspension system is modeled as a whole body (Cho *et al.*, 2005). When a vehicle suspension system has more DOFs, heavy online calculating load is needed and control response will lag. Thus a hierarchical control idea is come into being.

The idea of hierarchical control has been applied in many fields such as internet frameworks, power system control, etc. for a long time (Morin *et al.*, 1992; Chen *et al.*, 2004). Hagopian and Gaudiller (1999) introduced the hierarchical ideas into active control fields of a half vehicle suspension. In their method, a central control was proposed to take into account the pitch and the gap between the body and the ground, but they still employed conventional mathematic model. Masao and Tomohiro (1997) introduced a vehicle model where the suspension was treated as two independence systems for vibration analysis and control. The important aspects of the hierarchical control are how to divide each level and act a whole suspension system as many different 2-DOF suspension systems. Its key problem is how to decompose the sprung mass.

In this paper, a hierarchical modeling method is put forward. Here, the vertical and pitch accelerations of sprung mass center are adopted as center objects to harmonize local motions. Because the model is simplified, the online computer time is decreased evidently. Comparing with a passive case, the results show the validity and advantages of the method.

2. HIERARCHICAL MODELING

A motorcycle suspension with 5-DOFs is presented in Figure 1. In order to deduce the dynamic model of the system, it is divided into three dynamic balance stages in Figure 2. In the first stage, the front and rear suspension systems are controlled at position *I*, respectively. In the second stage, two independent systems are connected and

*Corresponding author. e-mail: wulong@mail.xjtu.edu.cn

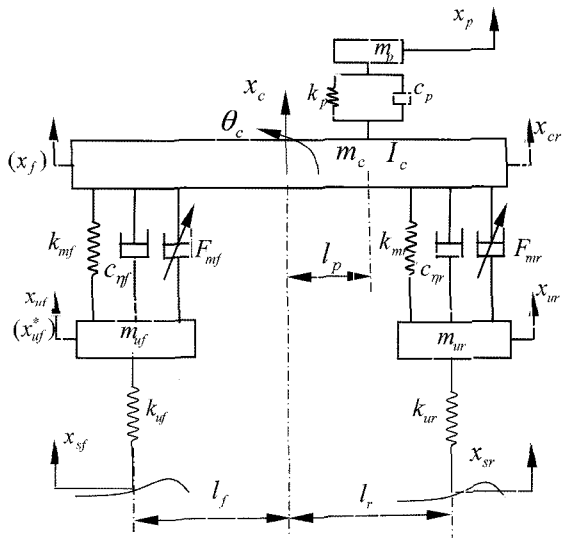

Figure 1. Motorcycle suspension model with 5-DOFs.

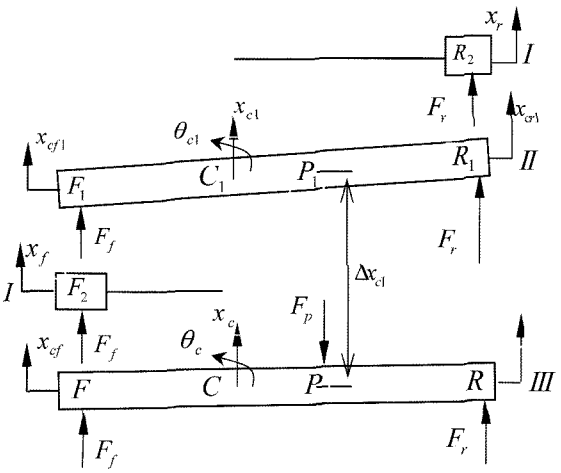

Figure 2. Hierarchical modeling course.

influenced mutually, and then moved to position *II*. In the final stage, the whole suspension must be moved to position *III* by considering the influence of driver-seat system. Because the position *III* is the final controlling position, it can be determined easily by the center level primely and the position *I* of front and rear suspension systems need to be studied based on the center level.

The motorcycle sprung mass is supported by the front and rear wheel systems which can be replaced by resultant forces F_f and F_r (including spring force, damping force, and semi-active actuating force). The driver-seat system contribute resultant force F_p (comprising spring force and damping force) to the suspension. See in Figure 3. Two dynamic equilibrium equations of force and moment can be given as follows.

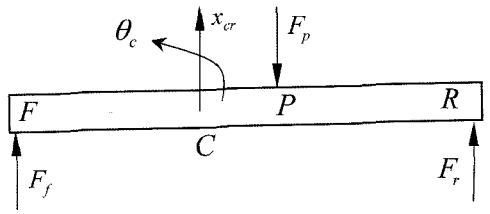

Figure 3. Force diagram of sprung mass.

$$m_c\ddot{x}_c=F_f+F_r-F_p \tag{1}$$

$$I_c\ddot{\theta}_c=F_rl_r-F_fl_f-F_pl_p \tag{2}$$

The Equation (1) is multiplied by l_p and combined by equation (2), the relation about F_f and F_r is

$$(l_f+l_p)F_f-(l_r-l_p)F_r=m_cl_p\ddot{x}_c-I_c\ddot{\theta}_c \tag{3}$$

Two relations between the vertical coordinates x_{cf} and x_{cr} and the sprung mass center vertical coordinate x_c are

$$x_c=x_{cf}+l_f\theta_c \tag{4}$$

$$x_c=(x_{cf}-l_r\theta_c) \tag{5}$$

Substituting equations (4) and (5) into equation (3), the relation of x_{cf} and x_{cr} can be obtained.

$$m_cl_p\ddot{x}_{cp}+m_cl_p\ddot{x}_{cr}+(m_cl_fl_p-m_cl_pl_r-2I_c)\ddot{\theta}_c -2(l_f+l_p)F_f+2(l_r-l_p)F_r=0 \tag{6}$$

In Figure 2, there is an obvious position change of the sprung mass from status *III* to *II* which shows the influence of a driver-seat system. Assuming Δx_{c1} is the displacement from point C to C_1, the following equations can be obtained.

$$x_{cf1}=x_{c1}-l_f\theta_{c1}=x_c+\Delta x_{c1}-l_f\theta_{c1} \tag{7}$$

$$x_{cr1}=x_{c1}-l_r\theta_{c1}=x_c+\Delta x_{c1}-l_r\theta_{c1} \tag{8}$$

There are two dynamic equilibrium equations for forces and moments with regard to mass center point C_1.

$$m_c\ddot{x}_{c1}=F_f+F_r \tag{9}$$

$$I_c\ddot{\theta}_{c1}=F_rl_r-F_fl_f \tag{10}$$

The influences of the driver-seat system are give as follows.

$$m_c\Delta\ddot{x}_{c1}=F_p \tag{11}$$

$$I_c(\ddot{\theta}_{c1}-\ddot{\theta}_c)=F_pl_p \tag{12}$$

Furthermore, the dynamic equilibrium equation of driver-seat system is

$$m_p\ddot{x}_p=c_p(\dot{x}_c+\dot{\theta}_cl_p-\dot{x}_p)+k_p(x_c+\theta_cl_p-x_p)=F_p \tag{13}$$

Substituting equations (7) and (8) into equations (9) and (10), we can get the force and moment equations at position *II*.

$$m_{cf\cdot f}\ddot{x}_{cf1}+m_{cr\cdot f}\ddot{x}_{cr1}=F_f+F_r \tag{14}$$

$$m_{cr\cdot m}\ddot{x}_{cr1}l_r-m_{cf\cdot m}\ddot{x}_{cf1}l_f=F_f l_f+F_r l_r \tag{15}$$

Here, $m_{cf\cdot f}=m_c l_r/l$, $m_{cr\cdot f}=m_c l_f/l$, $m_{cf\cdot m}=I_c/(l\cdot l_f)$, and $m_{cr\cdot m}=I_c/(l\cdot l_r)$. Subscript f or m denotes the concentrated mass expressed by force or moment form.

The two equations above indicate that the sprung mass could be simplified into a rigid pole without mass and two concentrated mass at its both ends. At the same time, the equations can be used to decompose a motorcycle suspension because it has only front and rear forces and accelerations. Furthermore, equation (14) shows that a motorcycle suspension system could be divided into two 2-DOF suspension systems directly according to the definition of allocation proportion when l_f is equal to l_r (Huang and Chen, 2003; Yu, 2000). Usually, l_f is unequal to l_r. Hence equation (14) and equation (15) provide a comprehensive and valuable method to solve this kind of problem.

Without the rear restriction, the concentrated mass of front suspension would move from point F_1 to F_2. Defining Δx_f is the distance from point F_1 to F_2, there would be a relation for Δx_f.

$$\Delta x_f=x_{cf1}-x_f \tag{16}$$

$$m_{cf\cdot f}\ddot{x}_f=F_f+m_{cf\cdot f}\Delta\ddot{x}_f \tag{17}$$

Similarly, defining Δx_r is the distance from point R_1 to R_2, we could obtain

$$\Delta x_r=x_r-x_{cr1} \tag{18}$$

$$m_{cr\cdot f}\ddot{x}_r=F_r-\Delta\ddot{x}_r \tag{19}$$

Substitute equations (16)-(19) into equations (14) and (15), the accurate expressions about Δx_f and Δx_r are obtained.

$$\Delta\ddot{x}_f=\left(\frac{1}{2m_c}-\frac{l}{2m_c l_r}-\frac{l_r^2}{2I_c}\right)F_f+\left(\frac{1}{2m_c}-\frac{l_f l_r}{2I_c}\right)F_r \tag{20}$$

$$\Delta\ddot{x}_r=\left(\frac{1}{2m_c l_f}-\frac{l}{2m_c}-\frac{l_r^2}{2I_c}\right)F_r-\left(\frac{1}{2m_c}+\frac{l_f l_r}{2I_c}\right)F_f \tag{21}$$

When the front and rear suspension sprung masses are displaced, the unsprung masses are also displaced and generate displacement variables Δx_{uf} and Δx_{ur}, respectively.

$$\Delta x_{uf}=x_{uf}-x_{uf}^* \tag{22}$$

$$\Delta x_{ur}=x_{ur}-x_{ur}^* \tag{23}$$

where x_{uf} and x_{ur} denote the unsprung mass displacements of front and rear suspension before decomposing, respectively. The x_{uf}^* and x_{ur}^* denote the unsprung mass displacements after decomposing, respectively. When the two dynamics equations representing the unsprung mass states of the front suspension system before and after decomposing are subtracted mutually and substituted by equations (16) and (22), the unsprung mass displacement Δx_{uf} of the front suspension would be obtained.

$$m_{uf}\Delta\ddot{x}_{uf}+c_{\eta f}\Delta\dot{x}_{uf}+(k_{mf}+k_{uf})\Delta x_{uf}=c_{\eta f}\Delta\dot{x}_f+k_{mf}\Delta x_f \tag{24}$$

In the same way, the unsprung mass displacement variable of the rear suspension can be obtained.

$$m_{ur}\Delta\ddot{x}_{ur}+c_{\eta r}\Delta\dot{x}_{ur}+(k_{mr}+k_{ur})\Delta x_{ur}=c_{\eta r}\Delta\dot{x}_r+k_{mr}\Delta x_r \tag{25}$$

The detailed implementation of the hierarchical modeling method for a motorcycle suspension is as follows.

1) The mathematical expectation of $\ddot{x}_c$ and $\ddot{\theta}_c$ by virtue of the road excitation should be determined firstly. The given range of $\ddot{x}_c$ and $\ddot{\theta}_c$ have their probabilities that will not exceed 99.7 percent of the limited values σ_s and σ_p, respectively. We require

$$\ddot{x}_c\le 1/3\,\sigma_s \qquad \ddot{\theta}_c\le 1/3\,\sigma_p \tag{26}$$

where σ_s and σ_p are the limited values of the vertical and pitch accelerations and can be pr-estimated.

$$\sigma_s=0.6x_s(t)\cdot u^2/l^2 \tag{27}$$

$$\sigma_p=0.6\cdot(x_{sf}-x_{sr})\cdot u^2/l^3 \tag{28}$$

2) The expectation values of F_f, F_r, F_p, $\ddot{x}_{cf1}$ and $\ddot{x}_{cr1}$ can be calculated by equations (1)–(15). The expectation of Δx_f and Δx_r can be obtained by equations (20) and (21). Thus the front and rear expectation values of the decomposed sprung mass accelerations $\ddot{x}_f$ and $\ddot{x}_r$ can be determined.

3) With known expectation values of $\ddot{x}_f$ and $\ddot{x}_r$, a 2-DOF state space is set up. The state vector is $\mathbf{X_i}$.

$$\mathbf{X_1}=[\mathbf{x_1}\ \mathbf{x_2}\ \mathbf{x_3}\ \mathbf{x_4}]^T=[x_i-x_{ui}^*\ \dot{x}\ \ x_{ui}^*-x_{si}\ \dot{x}_{ui}^*]^T \tag{29}$$

The output vector is $\mathbf{Y_i}$.

$$\mathbf{Y_i}=[\mathbf{y_1}\ \mathbf{y_2}]^T=[x_1\ x_3]^T=[x_i-x_{ui}^*\ x_{ui}^*-x_{si}]^T \tag{30}$$

The state differential equation is

$$\dot{\mathbf{X}}_\mathbf{i}=\mathbf{A_i}\mathbf{X_i}+\mathbf{B_i}\mathbf{U_i}+\mathbf{G_i}\mathbf{W_i} \tag{31}$$

output equation

$$\mathbf{Y_i}=\mathbf{C_i}\mathbf{X_i} \tag{32}$$

where subscript denotes the front or rear suspension.

$$\mathbf{A_i}=\begin{bmatrix}-\frac{k_{mi}}{c_{\eta i}} & 0 & 0 & 0\\ 0 & 0 & 0 & 0\\ 0 & 0 & 0 & 1\\ \frac{k_{mi}}{m_{ui}} & \frac{c_{\eta i}}{m_{ui}} & \frac{k_{ui}}{m_{ui}} & \frac{c_{\eta i}}{m_{ui}}\end{bmatrix}\quad \mathbf{W_i}=\begin{bmatrix}\ddot{x}_i\\ \dot{x}_{si}\end{bmatrix}$$

$$\mathbf{B}_i=\begin{bmatrix}\frac{1}{c_{\eta i}}\\0\\0\\-\frac{1}{m_{ui}}\end{bmatrix}\quad \mathbf{G}_i=\begin{bmatrix}\frac{m_{ci}}{c_{\eta i}}\\1\\-1\\0\end{bmatrix}\quad \mathbf{C}_i=\begin{bmatrix}1&0\\0&0\\0&1\\0&0\end{bmatrix}^T$$

Based on the output equation and an optimal control strategy, the actual control force F_{mi} can be determined. Then the true values of $\ddot{x}_f$ and $\ddot{x}_r$ are obtained.

4) The true variables $\ddot{x}_{cf}$, $\ddot{x}_{cr}$, F_f, F_r and F_p are determined according to the reverse procedure. The true values of $\ddot{x}_c$ and $\ddot{\theta}_c$ are realized.

3. NUMERICAL SIMULATION

3.1. The Semi-active Actuator

In this paper, the semi-active actuator is magneto-rheological damper shown in Figure 4. It was designed for motorcycle. Figure 5 shows some curves of the displacement vs. force. Here the amplitude of vibration is 0.02 m and the frequency is 2 Hz.

3.2. Road Profile

Because the harmonic superposition method is a high-fidelity conversion in time domain, this paper adopts it to form road excitation. Supposing that the effective frequency range ($f_{\min}$, $f_{\max}$) is divided into n subsections. The power spectrum density (PSD) of each subsection is

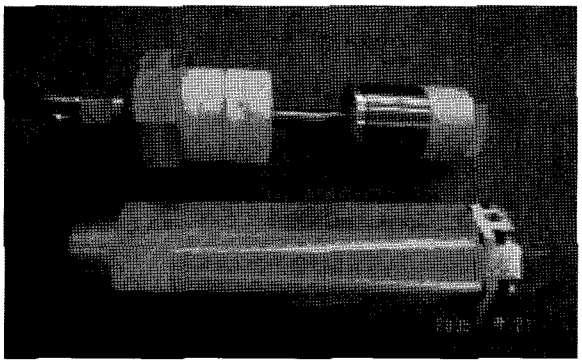

Figure 4. The magneto-rheological damper.

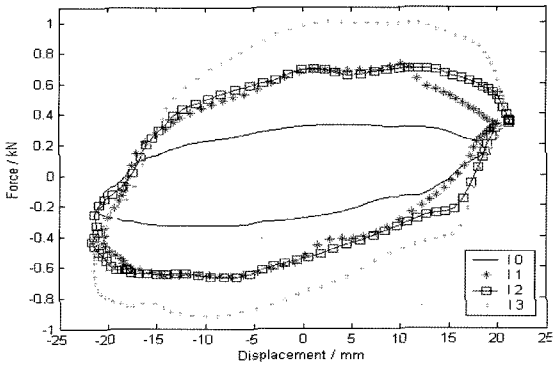

Figure 5. The displacement-force graph under different current of the MRF damper.

according $G_q(f_{mi})$ to its central frequency f_{mi}(i=1, 2, ..., n; m means center). The road stochastic displacement input under front wheel is

$$x_s(t)=\sum_{i=1}^{n}\sqrt{2G_q(f_{mi})\cdot\Delta f_i}\cdot\sin(2\pi f_{mi}t+\theta_i) \tag{33}$$

where $G_q(f_{mi})$ are average PSD values, m^2/Hz; Δf_i are subsection intervals, Hz; t is time, sec; θ_i are independent random variables distributed evenly in the region $[0,2\pi]$.

When a motorcycle runs with constant velocity and its wheelbase l, the time delay from front to rear wheel would be $\Delta=l/v$. The road stochastic displacement input under rear wheel is

$$x_{st}=x_s(t+\Delta)=\sum_{i=1}^{n}\sqrt{2G_q(f_{mi})\cdot\Delta f_i}\cdot\sin[2\pi f_{mi}(t+\Delta)+\theta_i] \tag{34}$$

For a motorcycle modeling, the road excitation under the front wheel can be described by equation (33) and rear by equation (34). In this paper, C grade road is selected according to the eight non-planeness grades of International Road Standard. Here, the effective frequency range is from 0.153 to 39.309 Hz; n=5000; C grad road PSD $G_q(f_{mi})$ is 128~512×10^{-6} m^2/Hz; The velocity v=80 km/h and wheelbase l=1.46 m. Figure 6 and Figure 7 are road excitation displacements in time domain and its PSD

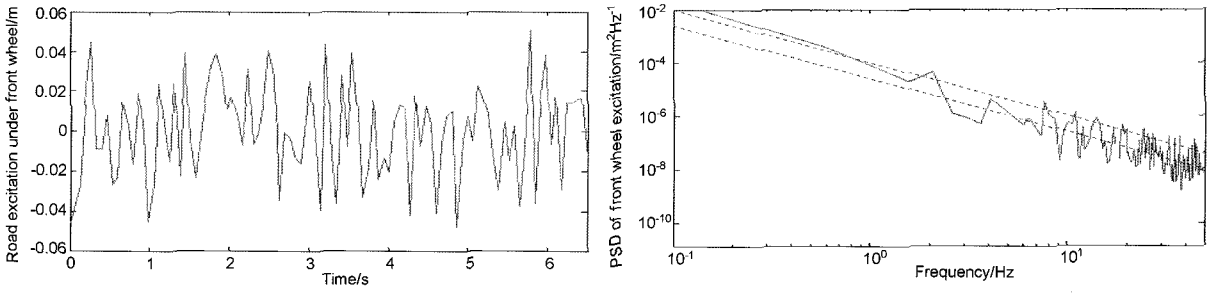

Figure 6. Road excitation displacement under the front wheel and its PSD.

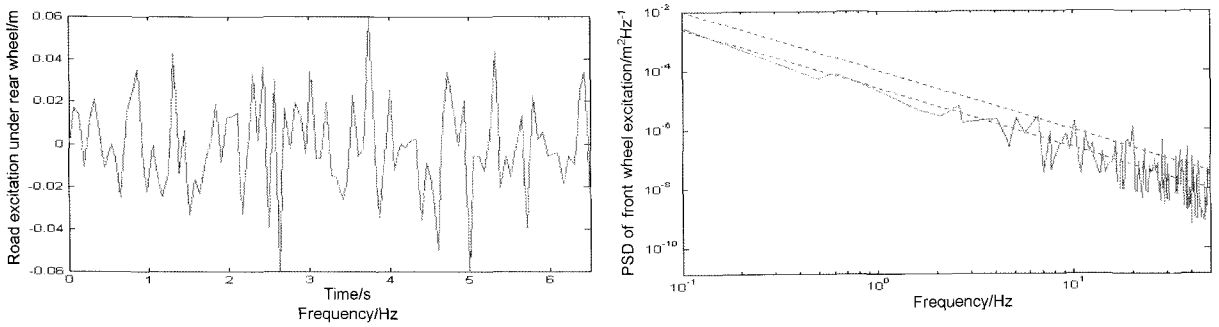

Figure 7. Road excitation displacement under the rear wheel and its PSD.

values, respectively. The dashed lines denote standard C grade road region in frequency domain. The figures show that the front and rear road excitations derived from the above equations meet with the practical requirements basically. Hence, it can be utilized in subsequent calculations.

3.3. Controller

In this paper, the function of controller is how to handle the input data. The controller comprises a center controller and two local controllers. According to the hierarchical modeling method, the responsibilities of center controller are: solve the expectation values of $\ddot{x}_f$ and $\ddot{x}_r$ according to the road data; determine the true values of $\ddot{x}_c$, $\ddot{\theta}_c$ and $\ddot{x}_p$ according to the true values of $\ddot{x}_f$ and $\ddot{x}_r$. Two local controllers are two parallel operators. They are responsible for solving the 2-DOF state spaces.

3.4. Simulation

In this paper, a motorcycle suspension with 5-DOFs is simulated for passive and semi-active control. The real time LQG method is employed for the front suspension. The wheelbase preview and LQG method are combined into control for the rear suspension (Marzbanrad *et al.*, 2004). The suspension parameters are as follows:

m_p=80 kg; k_p=1800 N/m; c_p=250 N·s/m; m_c=150 kg; I_c=80 kg·m^2; m_{uf}=25 kg; m_{ur}=25 kg; l_f=0.58 m; l_r=0.88 m; l_p=0.3 m; k_{tf}=180000 N/m; k_{tr}=220000 N/m; k_{mf}=7600 N/m; k_{mr}=40000 N/m; c_{rf}=750 N·s/m; c_{rr}=2000 N·s/m;

Assume the passive and semi-active suspension parameters are all the same except that the semi-active suspension has an additional control force. According to the center control equations and semi-active course, some presumptions must be set in advance as follows:

(1) The front and rear suspension deflections are limited in ±0.03 m that is the piston travel of MRF damper. The front and rear tire deformations are restricted to ±0.02 m.

(2) MRF damper output force changes from 200 *N* to 1000 *N*.

The sampling time is 0.02 second. The Matlab6.5 and Simulink4.0 compiler are utilized to simulate the system in a computer which has 1.0G CPU and 256M memory. Under the semi-active control, the weight numbers of the front suspension are 1000, 100000 and 0.0048, and the rear are 200, 100000 and 0. Some results are given from Figure 8 to 14. In these figures, real lines and dashed lines correspond to the semi-active and passive control results, respectively.

Figures 8 and 9 show the vertical acceleration of seat and sprung mass. Figure 10 gives the pitch acceleration of sprung mass. It is seen that the acceleration in the time and frequency domain under the passive control is higher than that under the semi-active control. The

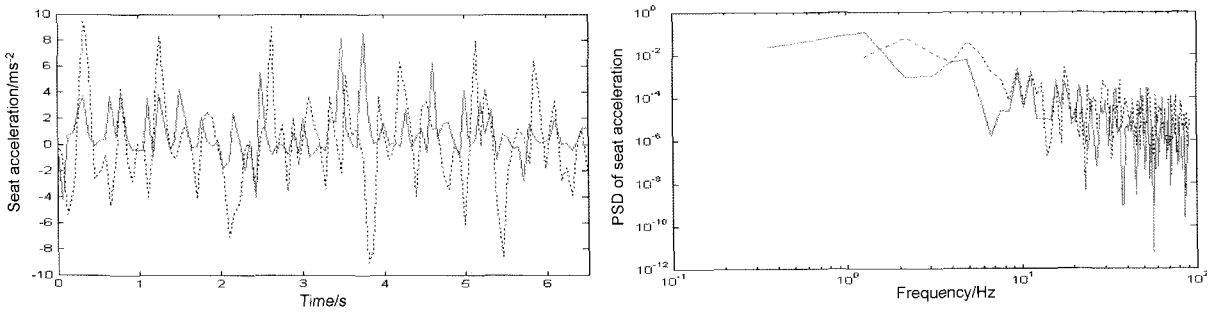

Figure 8. Seat vertical acceleration and its PSD. (real line denotes the results of semi-active control; dashed line denotes the results of passive control. latter graphs are the same as these except given annotation).

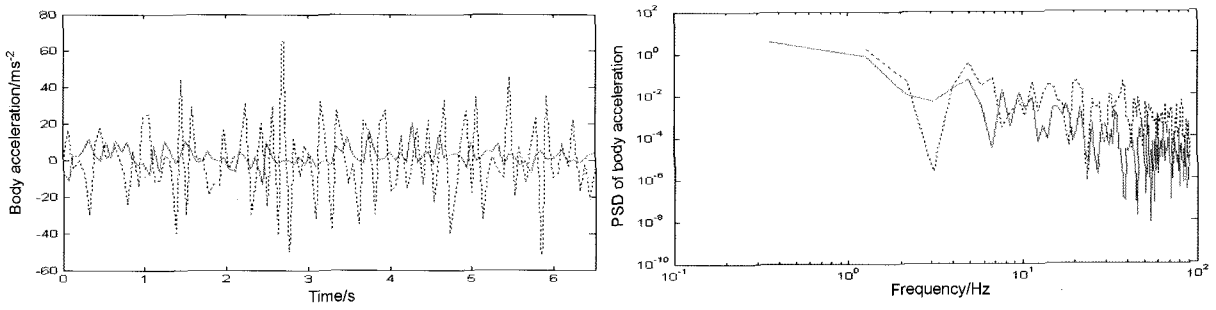

Figure 9. Body vertical acceleration and its PSD.

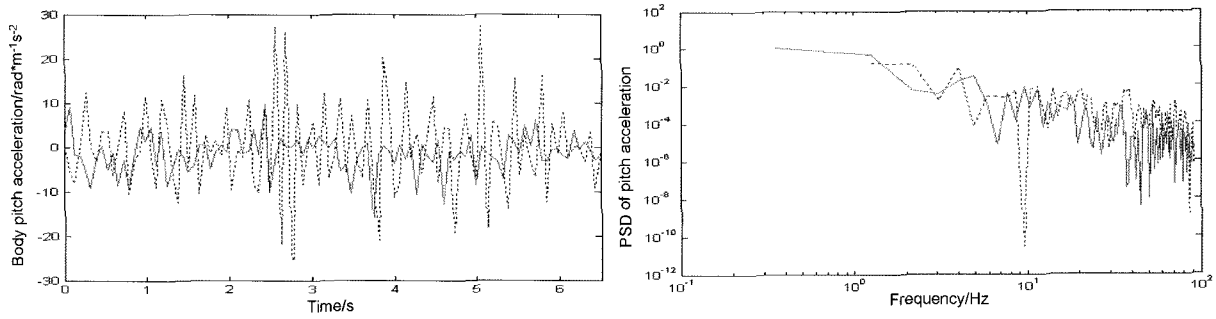

Figure 10. Body pitch acceleration and its PSD.

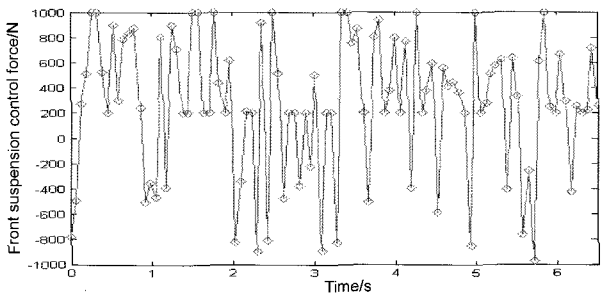

Figure 11. Output force of the front MRF damper.

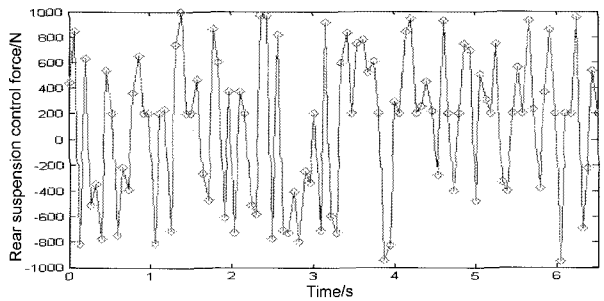

Figure 12. Output force of the rear MRF damper.

acceleration response near the body resonance is isolated effectively by using semi-active control. It can be seen that the control method in this paper can decrease body acceleration effectively not only at low but also at high frequency.

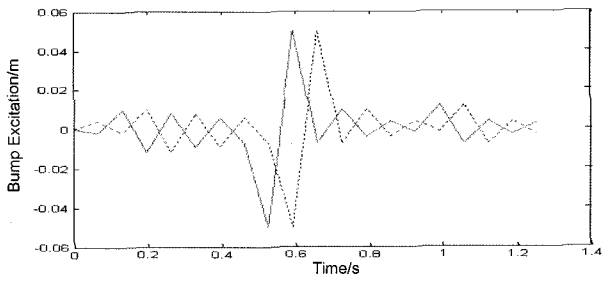

Figure 13. Bump excitation. (real line is the front side; dashed line is the rear side).

Figures 11 and 12 show the output forces of the front and rear MRF dampers under the semi-active control. It is seen that the control forces are averagely distributed between the minimum and the maximum outputs of the MRF damper. It indicates the weight numbers in this paper are suitable.

For the sake of testing ride comfort and handling performance further, a small bump is adopted and shown in Figure 13. All known conditions are the same as those given above and the amplitude of the bump is 0.05 m. Figure 14 shows the time histories of the bump responses of the seat, body vertical and pitch under passive and semi-active control. It is apparent that the semi-active suspension based on the hierarchical modeling method can significantly improve the deteriorated damping characteristics and reduce the vibration peaks.

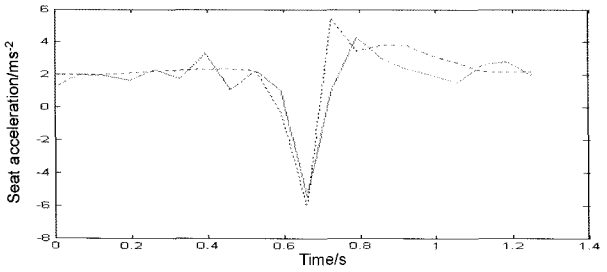

Figure 14. (a) Bump response of the seat vertical acceleration.

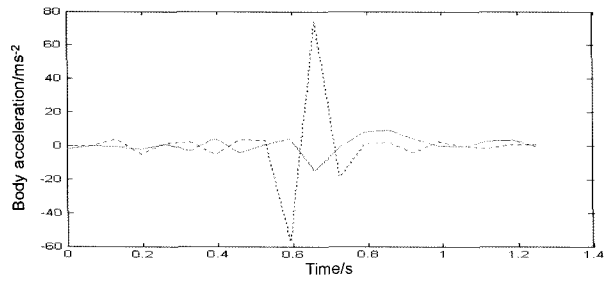

Figure 14. (b) Bump response of body vertical acceleration.

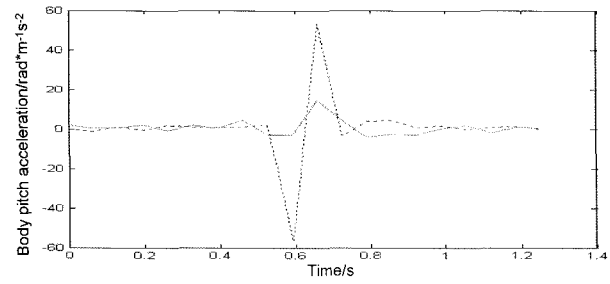

Figure 14. (c) Bump response of body pitch acceleration.

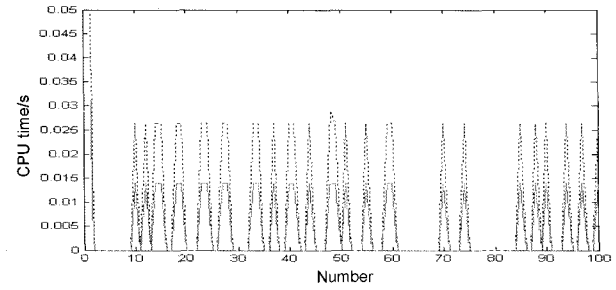

Figure 15. CPU time of online calculation. (real line is the hierarchical modeling method; dashed line is conventional method).

After employment of the hierarchical modeling method, only a quarter suspension computer time is needed because the calculations of the front and rear suspensions can be executed at same time. Figure 15 shows the CPU times to run a hundred cycles of the hierarchical modeling method in this paper and conventional method at same conditions. The total time of a hundred cycles employed by the hierarchical modeling method is 0.477 second and the conventional method is 0.901 second. We note that the value is reduced by 47.06% in the case of the hierarchical modeling method when compared with the conventional method.

From the simulation results above, it can be seen that the semi-active preview control based on the hierarchical modeling method given in this paper provides a better performance than the one under the passive control.

4. CONCLUSIONS

The primary purpose of this paper is to give a hierarchical modeling method which can translate a motorcycle suspension system with 5-DOFs into two 2-DOF suspension systems without special conditions. The conclusions can be drawn as follows.

(1) As a result of the decomposition and simplification of a motorcycle suspension, the online computer time is decreased. If the method is extended to multi-wheel vehicles, the complexity of the vehicle model could be simplified and the excessive online workload owing to more degrees of freedom would be avoided and the control effect can be improved.

(2) Two local 2-DOF suspension systems can be operated in parallel to decrease online computing time.

(3) According to the characteristics of hierarchical modeling method, different control strategies can be introduced to the two local 2-DOF suspension systems in order to obtain an effective control combination that can meet the practical requirements.

The hierarchical modeling method provides a new direction for a vehicle suspension control because of its characteristic to translate a complex suspension system into several 2-DOF suspension systems, and has a wide application in the field of off-road vehicle, military carrier and railway train.

REFERENCES

Chen, Z., Yan, W., Xu, Guoyu, and Wang, G. (2004). Hierarchical control theory and its application to power system automation. *Proc. IEEE Int. Conf.*, **2**, 643–646.

Cho, B. K., Ryu, G. and Song, S. J. (2005). Control strategy of an active suspension for a half car model with preview information. *Int. J. Automotive Technology* **7, 3,** 243–249.

Ericksen, E. O. and Gordaninejad, F. (2003). A magneto-rheological fluid shock absorber for an off-road motorcycle. *Int. J. Vehicle Design*, **33**, 139–152.

Huang, J. and Chen, L. (2003). A dynamic modeling

method of vehicle semi-active suspension with MR damper. *Precise Manufacturing & Automation*, **z1**, 17–19.

Marzbanrad, J., Ahmadi, G., Zohoor, H. and Hojjat, Y. (2004). Stochastic optimal preview control of a vehicle suspension. *J. Sound and Vibration,* **275,** 973–990.

Hagopian, J. D. and Gaudiller, L. (1999). Hierarchical control of hydraulic active suspensions of a fast all-terrain military vehicle. *J. Sound and Vibration*, **222**, 723–752.

Kok, J. J., Van Heck, J. G. G. A. M., Huisman, R. G. M. etc. (1997). Active and semi-active control of suspension systems for commercial vehicles based on preview. *Proc. American Control Conf.*, 206–215.

Masao, N. and Tomohiro, H. (1997). Vibration isolation analysis and semi-active control of vehicles with connected front and rear suspension dampers. *Society of Automotive Engineers of Japan,* **18**, 45–50.

Morin, M., Nadjm-Tehrani, S., Osterling, P. and Sandewall, E. (1992). Real time hierarchical control. *Software. IEEE,* **9**, 51–57.

Yu, Z. (2000). *Automobile Theory.* CMP (China Machine Press) Publishing Group. China. 126–128.

Zhang, Y. (2003). Time domain model of road irregularities simulated using the harmony superposition method. *Trans. Chinese Society of Agricultural Engineering*, **6**, 32–35.